Jordanian Journal of Engineering and Chemical Industries

Print ISSN: 2616 - 9584 Online ISSN: 2617 - 720X

Simulation and performance analysis of a Naphtha Hydrotreating (NHT) process using Aspen HYSYS

Hussam Elddin Nabeih Khasawneh*[1], Nada Al-Ananzeh[1] and Fares Abu Affan[2]

[1]Al-Balqa Applied University, Al-Huson University College, Chemical Engineering Department. PO Box 50, Al-Huson 21510, Irbid, Jordan
[2]Jordan University of Science and Technology, Chemical Engineering Department, P.O. Box 3030, Irbid 22110, Jordan

Abstract

This study presents a comprehensive simulation and analysis of a Naphtha Hydrotreating (NHT) unit, focusing specifically on the reaction section to evaluate operating conditions and enhance product quality using Aspen HYSYS® V12.1 (Aspen Technology, Inc.) simulation software. A continuous reactor model was developed to simulate the complex chemical transformations of C5–C12 paraffins, naphthenes, and aromatics. The methodology emphasizes the integration of catalytic reforming components and the calibration of separator logic to ensure thermodynamic consistency between the vapor and liquid phases. The findings indicate that precise management of the highly exothermic temperature rise during the initial hydrotreating (desulfurization) stage, followed by the management of the highly endothermic heat loss across the subsequent multi-bed catalytic reforming reactor system—typically operating between 280 and 425 °C—is critical for achieving deep desulfurization and optimal product yields. The results demonstrate that the simulated unit effectively reduces the sulfur content to less than 0.5 ppm, providing a technical framework for improving fuel quality, meeting environmental standards, and maximizing the recovery of high-purity hydrogen and light hydrocarbon by-products.

Paper type: Research Paper

Keywords: Naphtha, Simulation, Reheating, Refinery, Catalyst, Reactor

Citation: Khasawneh, H. E. N., Al-Ananzeh, N., and Abu Affan, F. "Simulation and performance analysis of a Naphtha Hydrotreating (NHT) process using Aspen HYSYS". *Jordanian Journal of Engineering and Chemical Industries*, Vol. **9**, No.2, pp:101-114 (2026). DOI: https://doi.org/10.48103/jjeci982026

1. Introduction

Currently, oil and its derivatives account for approximately 37% of global energy consumption and 90% of the fuel used in transportation systems (Mouler, 2025). The rapid growth in the utilization of and demand for crude oil across various industrial sectors has caused gasoline prices to increase due to higher-than-expected market demand (Dastnaei, 2025). However, the combustion of these fossil fuels results in the emission of particulate matter and hazardous gases, such as SOx and NOx, which contribute to severe environmental degradation. Sulfur represents one of the primary contaminants in petroleum products, directly contributing to the formation of solid particulates (soot) and gaseous SOx during combustion. Furthermore, the presence of even trace amounts of sulfur in engine fuels can poison and deactivate catalytic converters, severely compromising their operational efficiency (Overhary, 2025). To mitigate the harmful effects of these emissions, stringent environmental laws and regulations have been enacted globally, requiring refineries to convert their derivatives into ultra-low-sulfur products (Pershima, 2025). For example, the United States Environmental Protection Agency (EPA) established new standards limiting the sulfur content for highway fuels, while regulations enforced by the

* Corresponding author: E-mail: h.khasawneh@bau.edu.jo ORCID: **0000-0001-8924-8632**
Received: 19 April 2026 Revised: 23 May 2026

Jordanian Journal of Engineering and Chemical Industries (JJECI), Vol.9, No.2, 2026, pp: 101-114. Accepted: 09 June 2026

Marine Environment Protection Committee (MEPC) of the International Maritime Organization (IMO)—specifically the MARPOL Annex VI Protocol—have drastically restricted sulfur limits for marine fuel oils (Padervand et al., 2019, 2021).

Meeting these strict regulatory demands presents a major challenge for modern refineries, especially as recoverable oil reservoirs approach their half-life and newly extracted heavy crude oils contain significantly higher levels of sulfur (Han et al., 2017). To produce high-quality, low-sulfur fuels from poor-quality feedstocks, refineries rely heavily on downstream upgrading, specifically Naphtha Hydrotreating (NHT) and catalytic reforming. The primary product of the catalytic reforming unit is high-octane gasoline, accompanied by valuable by-products such as high-purity propane, butane, and hydrogen gas, which is recycled to sustain refinery operations (Gandomi, 2024; Ghanbari Pakdehi et al., 2025). The general reactions driving this reforming process include:
(1) Cyclization combined with dehydrogenation of paraffin's and their conversion to aromatics.
(2) Dehydrogenation of naphthenic and their conversion to aromatics (Khasawneh, 2025).
(3) Hydro isomerization.
(4) Hydrocracking of heavy paraffins into lighter, branched paraffins.

Extensive research has been conducted over the past two decades to optimize these desulfurization and reforming processes. Various methodologies, ranging from the development of highly active catalysts to alternative non-hydrodesulfurization methods—such as oxidative (ODS), biological (Bio-DS), and extractive (EDS) desulfurization—have been explored to achieve ultra-low-sulfur specifications. In the realm of process optimization, continuous catalytic regeneration has proven highly efficient. The modeling of this continuous process was comprehensively investigated by Hu et al., who established vital frameworks for reactor simulation (Gavanaroudi, 2024). Distinct from reactor modeling, other research has focused on downstream enhancements; for example, Rahimpour et al. successfully utilized palladium-silver membrane separation technology to continuously remove hydrogen gas, thereby shifting the thermodynamic equilibrium toward higher product yields (Khosravanipour Mostafazadeh & Rahimpour, 2009). To further advance and optimize these complex units, computational simulation has become an indispensable engineering tool. Simulation allows engineers to analyze the complex thermodynamic and kinetic behavior of chemical processes without the massive cost, risk, and time required for pilot-scale experiments. In NHT units, operating conditions such as temperature, pressure, the hydrogen-to-hydrocarbon ratio, and catalyst activity strongly affect reaction pathways and product quality (Samimi & Zarinabadi, 2012). Consequently, process simulators such as Aspen HYSYS provide a reliable framework for predicting process performance under varying feed qualities, facilitating rigorous sensitivity analyses. Because this computational method is rapid and highly accurate, it allows for comprehensive virtual testing prior to implementing physical plant modifications, thereby reducing fixed investment and operational costs, creating greater flexibility in design, and significantly improving overall plant safety.

The reforming process consists of two operational parts, which include:
(1) Feed Purification (Hydrotreating): Removal of feed impurities using hydrogen. In this part, the feed leaves the converter and mixes with hydrogen, then passes through a heat exchanger, where its temperature is increased to about 360 °C by indirect heat exchange. The heated mixture then enters the purification reactor (operating at approximately 30 atm). After purification, the stream enters a two-phase separator where light gases and hydrogen are removed. The liquid stream is then sent to the separation tower to remove the remaining gases, and the purified feed is finally routed to the reforming section (Kumar et al., 2017).
(2) Reforming Section: In the reforming section, the purified feed is mixed with recycled hydrogen and after passing through the first furnace and reaching the desired reaction temperature, it enters the primary reactor, where it undergoes rapid kinetic reactions, specifically dehydrogenation and hydro isomerization. Due to the high endothermic nature of these reactions, the temperature drops rapidly and they enter the second furnace and then the next reactor, so that the cyclization and hydrocracking reactions are carried out (Noorpoor & Mazare, 2018). After this stage, the feed enters the third furnace and the third reactor, and the hydrocracking and cyclization reactions are carried out again (Imanzadeh, 2024). After this stage, the feed enters the two-phase separator, and the feed is divided into two liquid and gas phases. The main part of the gas phase is hydrogen, and the liquid part enters the stabilization column and exits from the top of the C4 hydrocarbon column down and from the bottom of the stabilized gasoline column (Samimi, 2025).
In **Table 1**, focused on simulation and closely related modeling for Naphtha Hydrotreating (NHT) or Gasoline/ Naphtha HDS. All entries are in English and include the core method, software, and why each study matters for NHT simulation.

Table 1. Summary of Relevant Simulation and Modeling Studies for Naphtha Hydrotreating (NHT) and Hydrodesulfurization (HDS).

Ref	Methods / Model	Key Findings	Relevance to NHT Simulation
(Al-Ananzeh et al., 2025)	Process simulation + sensitivity analysis (T, P, H2/feed, catalyst, reactor diameter)	Identified optimal ranges (≈280–310 °C; ≈28.5 bar) and operating trade-offs; paired with exergy analysis of the unit train in related materials.	Direct NHT modeling with actionable operating windows; a strong baseline case for validating your own HYSYS model.
(Mevawala et al., 2023)	Plant-wide steady-state model + energy analysis	Uses HYSYS to extract data for exergy assessment; shows where large irreversibility arises around hydrotreating/stripping systems.	Helps place an NHT model in a refinery context and quantify energy losses (e.g., heaters/strippers) adjacent to NHT.
(Khasawneh, Sharifi Tashnizi, et al., 2025) *	Documented HYSYS flowsheet and modeling steps	Provides a reproducible HYSYS setup (unit blocks/streams) for NHT; complements	Practical reference to structure your own HYSYS NHT flowsheet and sensitivity runs.
(Mahdiraji & Zarini, 2025)	Thermodynamic/exergy analysis based on HYSYS results	>50% of input exergy lost to environment; ≈32.7% irreversibility in stripper reported in study assets.	Though the base study began earlier, the openly available 2024 materials are widely cited in recent NHT simulation work; useful for benchmarking utility and column losses.
(Mehrdadian, 2025)	Data-to-model integration; co-processing workflows	Demonstrates linking experimental hydro processing data with Aspen models; workflows transferable to NHT kinetic calibration.	Guides how to integrate lab/plant data to tune an NHT simulation (rate constants, deactivation, cut properties).
(Samimi & Zarinabadi, 2011)	Survey of algebraic/ODE deactivation models (e.g., power-law activity, poison/coke models)	Catalogs deactivation forms and fitting strategies for incorporation into hydrotreater simulators.	Choose/fit an activity-decay model for NHT reactors (vital for long-run simulations and revamp studies).
(Samimi et al., 2019)	Structure-oriented lumping; reactors segmented into micro-segments	High-resolution molecular simulation captures hydrotreating effects across units; demonstrates reactor-segment modeling.	Offers an advanced path (beyond simple lumps) to represent NHT chemistry and product quality shifts.
(Khasawneh, Ameer, et al., 2025)*	Mechanistic/kinetic insights under hydro treating conditions	Clarifies competing reactions (diene → olefin; isomerization) relevant to octane retention in FCC naphtha hydro treating.	Inform your NHT kinetic set (e.g., diolefin saturation reactor ahead of main NHT) and octane-loss trade-offs.

The foundational flowsheet architecture and operational envelopes were adapted from established industrial benchmarks Ref (Al-Ananzeh et al., 2025; Samimi, 2025). To evaluate the thermal efficiency of the simulated unit, energy and exergy losses were strictly benchmarked across the heater and stripper components (Khasawneh, Sharifi Tashnizi, et al., 2025). Furthermore, to ensure the long-term predictive accuracy of the kinetic model, a catalyst deactivation law was embedded into the reaction kinetics (Samimi et al., 2019), and the overall system behavior was validated against comprehensive sensitivity analyses (Mehrdadian, 2025).

1.1. Effects of Sulfur on Diesel Engines and Emission Control Technology

Diesel engines are ideal for heavy-duty applications. They provide low-cost, long-lasting power for trucks, buses, and other off-road equipment, such as construction and agricultural machinery. Recent innovations in these engines have greatly increased their use. These advances, combined with lower fuel costs compared to gasoline-powered vehicles, have made diesel engines increasingly popular in a

variety of applications. Diesel engine exhaust is a complex mixture of gases, liquids, and particulates. These exhaust gases mainly contain particulate matter (PM) and nitrogen oxides (NOx), while the amounts of hydrocarbons (HC) and carbon monoxide (CO) present are much lower than in gasoline engines. Particulate matter is generally divided into three categories:
(1) Solids (carbon-based particles).
(2) Organic solvents (heavy hydrocarbons attached to carbon particles).
(3) Sulfates (formed from the oxidation of burned sulfur).

The amount of each of these three categories depends on the engine technology and the sulfur content of the fuel. The total quantity and mass of particulate matter emitted in diesel engine exhaust is significantly greater than the particulate matter produced in a well-maintained gasoline engine. In general, reducing the amount of sulfur reduces the amount of SO_2 produced and particulate matter in these engines. Vehicles equipped with diesel emission control technologies can separate pollutants from exhaust gases. As part of the emission control systems, these devices can convert or absorb pollutants before they enter the exhaust pipe. All types of these devices lose their proper efficiency to some extent with the presence of sulfur in the fuel (Samimi & Zarinabadi, 2011).
Figure 1 illustrates the negative effects of sulfur in diesel fuel on engine components and emission control technologies. The severity of impacts is shown on a negative scale (-1 to -5). The most critical effects are observed in SOx emissions, particulate matter (PM) emissions, and catalyst poisoning, while engine wear, DPF efficiency, and fuel economy are also significantly affected.

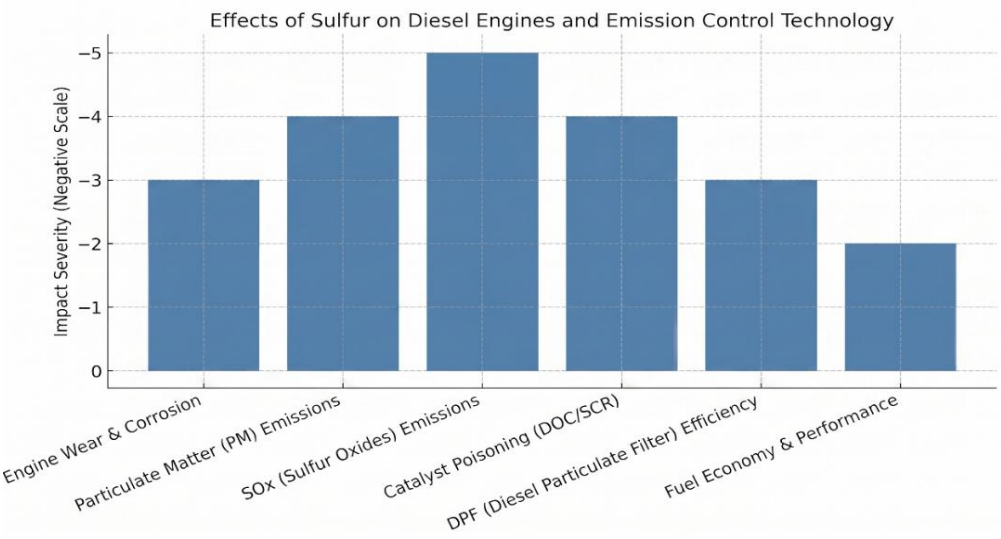

Fig. 1. Negative Effects of Sulfur in Diesel Fuel on Engine Components and Emission Control Technologies.

1.2. Regulatory Evolution and the Imperative for Deep Desulfurization

To reduce emissions of particulate matter (soot) and sulfur oxides, regulatory agencies have established strict guidelines to limit sulfur content in diesel fuel. In November 1990, the United States Environmental Protection Agency (EPA) mandated that by October 1993, all diesel-powered motor vehicles utilize fuel with a maximum sulfur content of 500 ppmw, classified as low-sulfur diesel (LSD) (Pershima, 2025; Samimi et al., 2019). In January 2001, these requirements were made more stringent. By early June 2006, the agency required refiners to reduce the sulfur content of highway motor fuels to 15 ppmw, establishing the standard for ultra-low-sulfur diesel (ULSD) (Khasawneh, Ameer, et al., 2025; Samimi et al., 2020). Consequently, by early December 2010, all diesel fuels used on highways were required to meet ULSD specifications. Additionally, distinct diesel fuel grades are utilized in non-road, rail, and marine transportation systems. Prior to 2004, the EPA did not set a specific limit for sulfur in non-road diesel fuel; however, industrial applications of this fuel type were exempted, and a baseline limit of 0.5 wt% (5,000 ppmw) was generally considered acceptable (Abubakar et al., 2020; Vakili, 2025).

The structural topology of the reforming unit must be established on the flowsheet prior to defining specific operating conditions. This sequential configuration is essential because the flowsheet architecture fundamentally dictates the direction of material flow, the precise connectivity between sequential units (e.g., from the preheater to the reactor, separator, and stripper), and the foundational paths required for accurate mass and energy balances. Process simulation software (such as Aspen HYSYS, Aspen Plus, or PRO/II) cannot mathematically assign temperatures, pressures, flow rates, or reaction parameters until the equipment is logically connected, since:
(1) Operating conditions are highly interdependent on upstream and downstream units.
(2) Pressure drops and energy flows must be calculated continuously along the material streams.

(3) Reactor temperatures and separator pressures must precisely reflect the actual process sequencing.
Consequently, placing the equipment on the flowsheet first allows the simulation engine to calculate consistent and thermodynamically converged operating conditions.

2. Materials and Methods

2.1 NHT Reactor Section

Importing the Component List and Fluid Package ensures that the simulation environment contains all real chemical components present in the NHT feed (e.g., C5–C12 paraffins, naphthenes, aromatics, sulfur compounds, and nitrogen compounds) and utilizes the correct thermodynamic models for phase behavior (e.g., Peng–Robinson, Soave–Redlich–Kwong, or specialized hydrocarbon packages). This is essential because accurate reaction prediction, phase equilibrium, separation behavior, and equipment calculations depend strongly on the correctness of the component definitions and the suitability of the equation of state for naphtha under a high-pressure hydrogen atmosphere. In short, without the correct component list and thermodynamic package, the simulation would not represent real NHT behavior.

The initial reaction section, consisting of the Naphtha Hydrotreating (NHT) unit, was developed and simulated within the Aspen HYSYS environment. To accurately model the phase equilibria and thermodynamic properties of the highly non-ideal hydrocarbon mixtures under a high-pressure hydrogen atmosphere, the Soave-Redlich-Kwong (REFSRK) thermodynamic fluid package was utilized.

While these terms are occasionally conflated in general literature, it is critical to explicitly distinguish between hydrodesulfurization (HDS) and Naphtha Hydrotreating (NHT) within the scope of this simulation. HDS refers strictly to the catalytic chemical reaction mechanisms specifically, the hydrogenolysis pathway where carbon-sulfur bonds are cleaved to form hydrogen sulfide (H_2S). In contrast, NHT represents comprehensive, feedstock-specific industrial unit operation. The NHT process encompasses not only the HDS kinetic reactions but also Hydrodenitrogenation (HDN), the saturation of reactive olefins, and the integrated thermodynamic separation infrastructure (e.g., high-pressure separators and stabilizer columns). Therefore, NHT is the overarching physical process required to transform raw naphtha into a purified reformate feed, utilizing HDS as its primary, but not exclusive, chemical mechanism.
Within this simulation framework, the reactor kinetics were explicitly defined to model both the HDS and HDN pathways to accurately capture the conversion of heterocyclic compounds. In the HDS reactions, sulfur-bearing molecules such as mercaptans, sulfides, and complex thiophenes undergo hydrogenolysis to form saturated hydrocarbons and hydrogen sulfide (H_2S). Concurrently, the HDN reactions target nitrogenous compounds (e.g., pyrroles and pyridines), reacting with hydrogen to yield saturated hydrocarbons and ammonia (NH_3). The deep desulfurization achieved in this unit—reducing the sulfur content to 0.5 mg/L—is a direct result of optimizing the hydrogen partial pressure and reactor temperature to push these highly exothermic reaction equilibria toward complete conversion. To sustain optimal hydrotreating kinetics and prevent premature catalyst coking, the molar ratio of recycle hydrogen to hydrocarbons was strictly maintained at 3.5.

Following the NHT processing and intermediate separation, the sweetened naphtha is routed to the reforming section. This section was modeled utilizing a Continuous Regeneration Catalytic Reformer (CCR) configured with a four-bed architecture. Feed properties entering the CCR were characterized using bulk properties derived from a standard ASTM D86 distillation profile and a PONA (Paraffins, Olefins, Naphthenes, Aromatics) basis, as detailed in **Table 2**.

Table 2. Feedstock Properties and Distillation Profile for the Continuous Catalytic Reformer (CCR).

Default	Feed Type
D86	Distillation Type
80	0% point (C)
90	5% point (C)
95	10% point (C)
108	30% point (C)
120	50% point (C)
133	70% point (C)
154	90% point (C)
160	95% point (C)
170	100% point (C)
Weight %	PONA Basis
40	Paraffins (%)
0	Olefins (%)
50	Naphthenes (%)
10	Aromatics (%)

Reactor operating parameters, including volumetric and mass flow rates, were specified in accordance with **Table 3**.

Table 3. Operating Parameters and Flow Specifications for the Reactor Section.

Pressure (Pa)	Temperature (°C)	Mass Flow (kg/h)
1155	425	1.8×10^5

The thermal profile across the multi-bed system was strictly managed; reference inlet temperatures and specified temperature drops across each reactor bed were defined to account for the highly exothermic desulfurization reactions followed by the highly endothermic reforming reactions, and all according to **Table 4**.

Table 4. Temperature Control Profile Across the Multi-Bed Reactor System (Reactor Inlet Reference Temperature = 520 °C).

Reactor Bed	Temperature Change, ΔT (°C)
R1 Temperature basis	0
R2 Temperature basis	-2.5
R3 Temperature basis	-3
R4 Temperature basis	-0.9

The active catalyst mass flow rate was defined at 850 kg/h to ensure adequate space velocity. Furthermore, the product pre-heating train was specified to deliver the feed at 120 °C and 820 kPa, establishing the requisite thermal boundary conditions prior to initial phase separation (Han, 2022).

To capture the conversion of heterocyclic compounds within the simulation, the reactor kinetics were explicitly defined to model both hydrodesulfurization (HDS) and hydrodenitrogenation (HDN) pathways. In the HDS reactions, sulfur-bearing molecules such as mercaptans, sulfides, and complex thiophenes undergo hydrogenolysis to form saturated hydrocarbons and hydrogen sulfide (H_2S). Concurrently, the HDN reactions target nitrogenous compounds (e.g., pyrroles and pyridines), reacting with hydrogen to yield saturated hydrocarbons and ammonia (NH_3). The deep desulfurization achieved in this unit—reducing the sulfur content to 0.5 mg/L—is a direct result of optimizing the hydrogen partial pressure and reactor temperature to push these exothermic reaction equilibria toward complete conversion.

2.1 Optimization Procedure and Parametric Analysis

A rigorous parametric optimization methodology was established within the Aspen HYSYS simulation environment to successfully reduce the naphtha sulfur content to the ultra-low specification of < 0.5 ppm. Rather than relying on external stochastic solvers, the optimization framework was systematically driven by deterministic sensitivity analyses and the precise calibration of internal logical constraints (e.g., 'Set' operations) to ensure strict thermodynamic consistency throughout the process. The procedure evaluated key operational decision variables, specifically tuning the reactor thermal profile (280–425 °C), the system operating pressure, and the hydrogen-to-hydrocarbon recycle ratio, which was optimally anchored at 3.5

This multiparametric objective was governed by two critical boundary constraints: (1) maximizing the kinetic cleavage of carbon-sulfur bonds via the HDS pathway to satisfy stringent environmental specifications, and (2) strictly maintaining the hydrogen partial pressure below the thermodynamic activation threshold for aromatic hydrogenation, thereby preserving the reformate's high-octane value. By iteratively mapping these decision variables against overall product yield and the separation efficiency of acid gases (H_2S and NH_3) across the downstream high-pressure flash units, an optimized, thermodynamically stable operating envelope was successfully delineated and validated.

3. Results

3.1 Reactor Settings and Effluent Processing

The steady-state simulation successfully converged, enabling a comprehensive evaluation of the unit's operational parameters. Following the reactor section ([Reformer-100], **Figure 2**), the effluent streams ([Net H2], **Figure 3**) and ([Net Liq], **Figure 3**) were combined ([MIX-100], **Figure 3**) and routed to a primary two-phase product separator ([V-100], **Figure 2**) operating at 32 °C and 820 kPa (**Figure 2**).

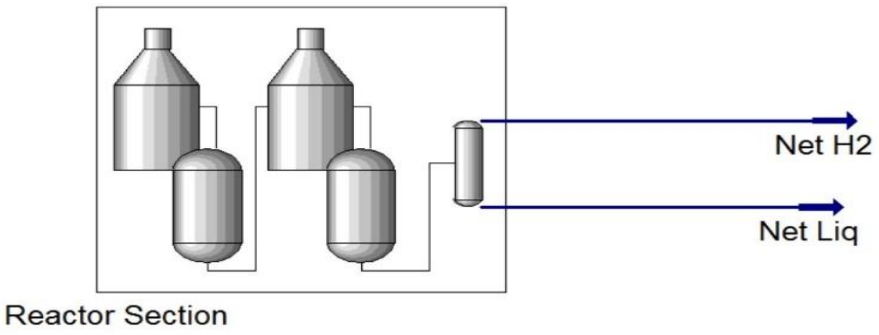

Fig. 2. Aspen HYSYS Flowsheet of the Reactor Section.

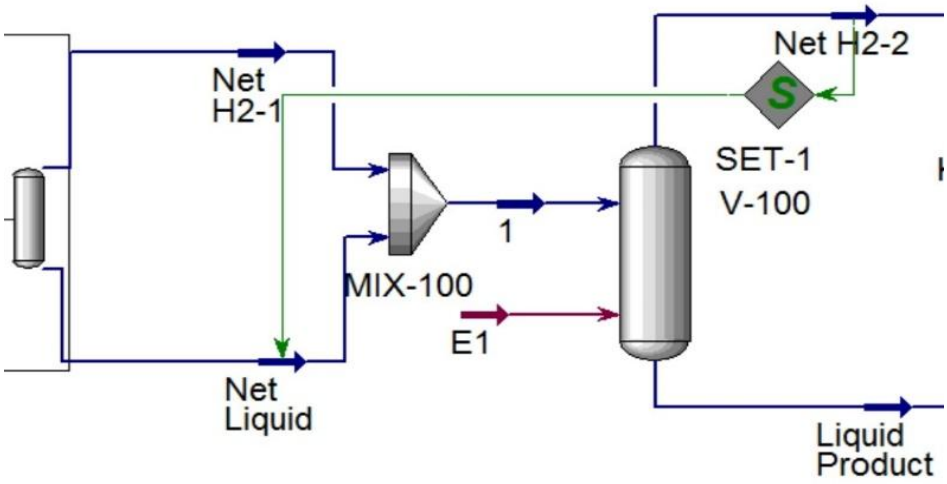

Fig. 3. Implementation of Logical 'Set' Operations for Isothermal Vapor-Liquid Equilibrium (VLE).

To accurately track the mass balance of the system, the subsequent routing of these separated phases is delineated below:

Top Vapor Effluent Path: The hydrogen-rich gas stream ([Net H2-2], **Figure 4**) exiting the top of the primary separator ([V-100], **Figure 3**) underwent compression to 230 kPa and was intercooled to 30 °C prior to entering a secondary three-phase separator ([V-101], **Figure 4**), which was designed to drop out residual heavy condensable. To close the recycle loop without utilizing a mathematically intensive recycle operator, a secondary 'Set' function ([SET-2], **Figure 4**) perfectly equalized the pressures of the recycled hydrogen vapor and the upstream system integration points, successfully isolating the high-purity hydrogen by-product.

Bottom Liquid Effluent Path: Conversely, the primary stabilized liquid stream ([Liquid Product], **Figure 4**) exiting the bottom of the first separator ([V-100], **Figure 3**) was pressurized to 570 kPa via a centrifugal pump ([P-100], **Figure 4**). This pressurized liquid was subsequently combined with the secondary liquid condensate recovered from the three-phase separator. Merging these streams under strict isobaric conditions generated a single, homogenized intermediate reformate feed ([Net Reformate], **Figure 6**), preventing phase instability and optimizing the hydraulic load for the downstream fractionation sequence.

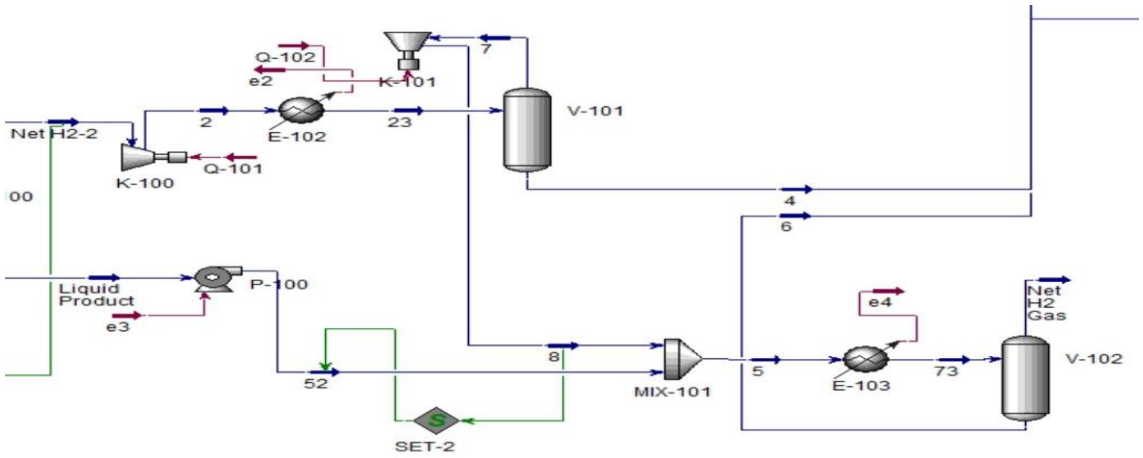

Fig. 4. Implementation Process Flow Diagram of the Intermediate Phase Separation and Hydrogen Recycle Loop.

3.2 Downstream Fractionation and Stabilization

Prior to deep fractionation, the combined reformate stream (Net Reformate, **Figure 6**) was preheated to 140 °C. The primary distillation column (stripper) (T-100, **Figure 6**) was configured with 29 theoretical stages, with the feed stage optimally located at tray number 15. The column utilized a partial condenser operating at 120 kPa and a reboiler at 145 kPa, operating at a reflux ratio of 1.8. To resolve the column's degrees of freedom and force convergence toward the desired light-ends removal, internal temperature constraints were applied, specifically anchoring the sixth tray at 120 °C (**Figure 5**).

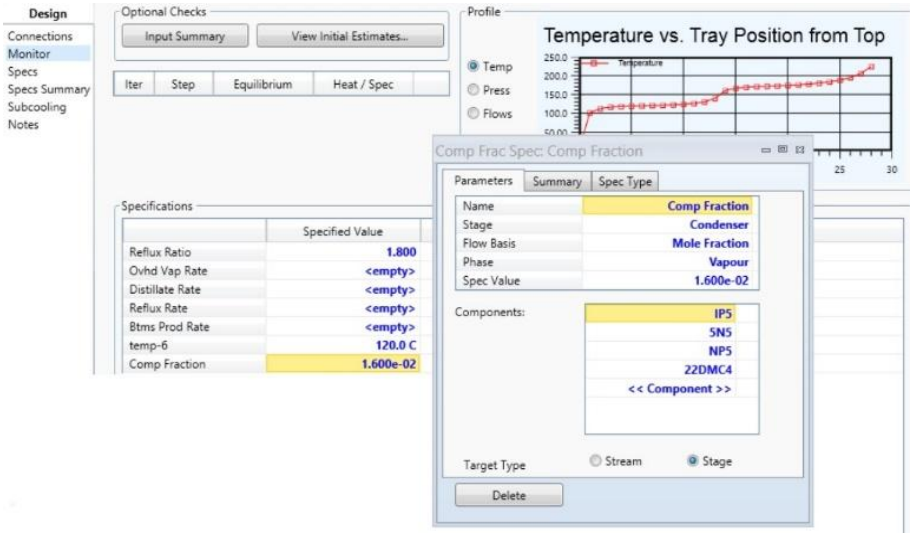

Fig. 5. Distillation Column Specifications and Internal Temperature Constraints.

The stabilized bottom product from the primary column (T-100 bottoms, **Figure 6**) was thermally conditioned to 140 °C before introduction to the secondary distillation fractionator (T-101, **Figure 6**). This unit, comprising 35 theoretical stages with a feed inlet (T-101, **Figure 6**) at tray 19, operated with a total condenser at 132 kPa, a reboiler at 196 kPa, and a reflux ratio of 0.5. Full system convergence for this final purification step was achieved by constraining the third tray temperature to 118 °C, which computationally ensured the heavy reformate product successfully met the stringent ultra-low sulfur specification of less than 0.5 ppm. The comprehensive simulation map encompassing the entire reforming and stabilization complex is illustrated in (**Figure 6**).

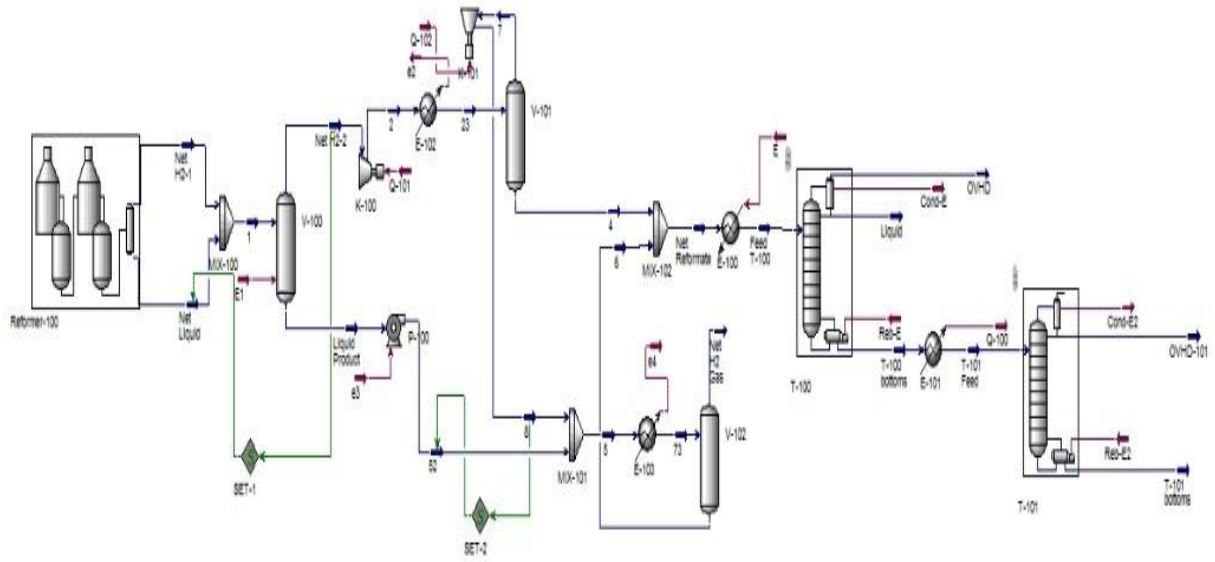

Fig. 6. Comprehensive Aspen HYSYS Simulation Flowsheet of the Reforming and Stabilization Complex.

In most NHT high-pressure separators, the vessel operates nearly isothermally because: (1) vapor–liquid equilibrium (VLE) occurs at a single temperature corresponding to the given pressure; (2) no significant heat exchange occurs inside the vessel; and (3) both the gas and liquid phases leave the separator at the same equilibrium temperature. If these temperatures differed, thermodynamic inconsistencies would arise, causing equilibrium calculations to fail. Thus, maintaining equal outlet temperatures ensures that the system reflects true VLE and that the simulation results remain accurate and physically valid.

Following the reactor effluent cooling train, the removal of the resulting byproducts (H_2S, NH_3, and H_2O) is systematically executed to prevent downstream catalyst poisoning and corrosion. Wash water is continuously injected upstream of the high-pressure cold separator to dissolve the generated NH_3 and a portion of the H_2S, forming an aqueous ammonium bisulfide (NH_4HS) solution, which is continuously drawn off. The remaining unreacted hydrogen and light vaporized H_2S are flashed off as overhead gas. The resulting liquid effluent from this separator—comprising the treated naphtha, residual light hydrocarbons, and trace dissolved sour gases—is systematically cooled to 140 °C prior to entering the distillation (stabilizer) column (T-102, **Figure 6**). This thermal conditioning is a critical operational parameter necessary to establish the precise thermodynamic conditions required for efficient fractionation. By regulating the feed temperature to this established optimum, the stabilizer column maintains a balanced vaporization-condensation profile. Utilizing the bottom reboiler, the residual H_2S, moisture, and light ends (C1-C4) are completely stripped and routed to the overhead receiver. This prevents hydrodynamic instabilities, minimizes the energy load, and ultimately yields a rigorously sweetened naphtha at the column bottoms, fully prepared for the downstream reforming unit.

4. Discussion

4.1 Downstream Stabilization Process Operation

Towers are much larger in diameter than atmospheric towers, typically 12 to 15 meters. Operating pressure is maintained by means of steam ejectors and condensers. The size and number of units are determined required and the quality of the vapors used; for 25 mmHg, three stages of ejectors are usually required. Reducing the pressure drop induction unit and the flash zone by a few millimeters saves operating costs. In standard real refinery operations, the distillation capacity provided is 80,000 barrels per day (about 4 million tons per year) with a fuel consumption of about 3,200 MMBtu per day.

heavy residual feedstocks undergo rigorous thermal fractionation to recover valuable intermediate distillates, such as naphtha, kerosene, and diesel. To prevent the thermal degradation of these complex hydrocarbon mixtures and maintain operational integrity, the process thermodynamics—specifically the pressure and temperature profiles—must be strictly controlled. Given the substantial economic premium of lighter distillates over heavy residual compounds, refining configurations are continuously optimized to maximize the recovery of these high-value fractions. The efficiency of this separation process and the resulting product distribution are graphically represented by the yield curve in (**Figure 7**).

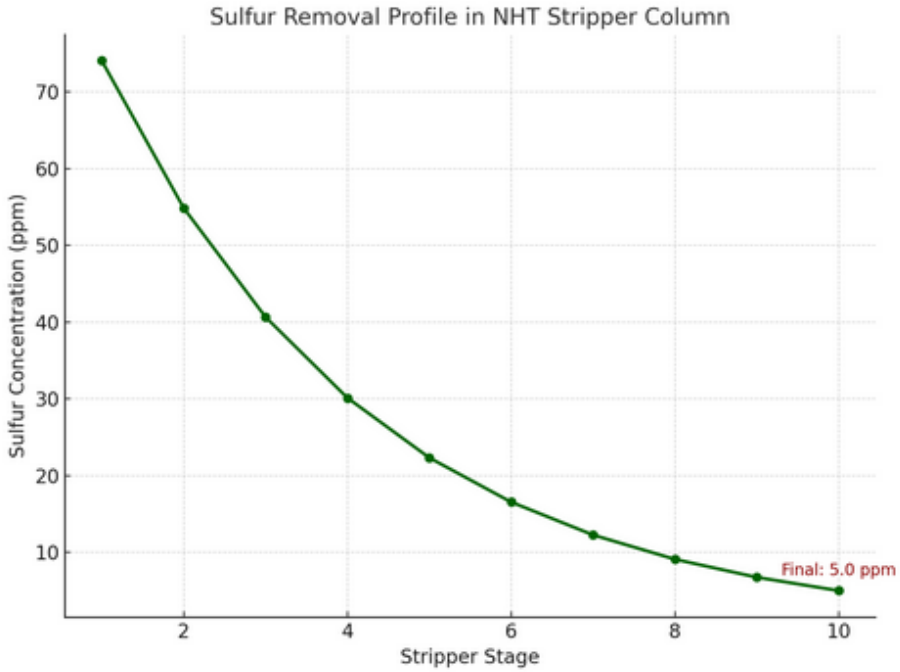

Fig. 7. Sulfur Removal Profile Across the NHT Stripper Column Stages.

Figure 7 illustrates how sulfur concentration decreases progressively across the stripper stages, highlighting the efficiency of sulfur elimination in the reaction/stripping section.

4.2 Operating Conditions of the Atmospheric Distillation Tower

The temperature of crude oil entering the furnace is between 200-280 °C, and then inside the furnace this temperature will reach 330-370 °C. The operational pressure is strictly maintained at 101.3 kPa to ensure phase stability. The principle of operation of this tower is based on the difference in the boiling point of the materials. Each oil cut possesses a specific boiling point range, and it can be removed from the tower across that temperature range. Accordingly, light compounds are removed from the top of the tower and heavier compounds from the bottom of the tower.

The feed, which has reached the desired temperature in the furnace, enters the tower. Approximately the middle trays are the feed inlet, although its optimal location can vary depending on the conditions. After the feed enters, liquids move downwards and gases move upwards. Light compounds exit from the top of the tower and enter a condenser where they are partially or completely condensed. The reflux will enter the tower from above. The temperature of the distillation tower increases from top to bottom. On the other hand, the compounds existing at the end of the tower are in liquid form and after passing through a Reboiler, they enter the tower as gas. The purpose of doing this is to create the maximum concentration difference between the gas and liquid streams in the distillation tower, which increases the separation efficiency.

4.3 Mass Transfer Fundamentals

In general, distillation columns operate based on the fundamental principles of mass transfer. In a mass transfer process, the driving force that transfers mass from one phase to another—assuming temperature and pressure remain constant—is the concentration gradient. Inside the distillation column, there are several horizontal trays where the vapor and liquid phases come into direct contact. With valid approximation, the temperature and pressure can be considered nearly constant across each tray, allowing the difference in concentration to dictate the mass transfer. The greater this difference, the higher the rate and extent of mass transfer. The introduction of a light liquid stream from the top of the column and a heavy vapor stream from the bottom is continuously executed to facilitate this precise purpose

4.4 Thermal Cracking Parameters

Thermal cracking involves a chemical cracking process followed by physical separation principles (based on boiling point differences) to isolate the desired products. The products of this process generally include fuel gas, naphtha, gas oil, and cracking residues. To achieve the necessary operating conditions to destabilize larger hydrocarbons, a temperature of approximately 450–500 °C and a pressure of 2–3 bar is typically maintained.

4.5 Hydrogen Treatment and Desulfurization

Many crude oils contain a high concentration of sulfur, which is a highly undesirable contaminant that severely degrades the quality of the final products. Therefore, the distillates produced from the atmospheric and vacuum distillation columns are treated with hydrogen so that the sulfur is ultimately removed as hydrogen sulfide (H_2S). The hydrogen required for this is supplied from the downstream reforming unit.
The specific operating conditions of hydrotreaters depend on the characteristics of the feedstock. For a naphtha feed, the reactor temperature is typically maintained between 280 and 425 °C, and the pressure is set between 200 and 800 psig. The primary chemical reactions occurring in this unit are as follows:

$$R\text{-}SH + H_2 \rightarrow R\text{-}H + H_2S \text{ (catalyzed at elevated temperatures)}$$
$$H_2S + NaOH \rightarrow NaSH + H_2O$$

While the Naphtha Hydrotreating (NHT) simulation successfully models the extraction of hazardous byproducts (H_2S and NH_3) from the hydrocarbon phase, the ultimate chemical neutralization of these toxic gases occurs outside battery limits (OSBL) of this specific unit. For instance, the neutralization of hydrogen sulfide via the caustic scrubbing reaction shown above is a downstream environmental operation. It is critical to note that the resulting sodium bisulfide (NaSH) does not remain in this hazardous state. This spent caustic solution is strictly routed to an external Spent Caustic Treatment Unit (SCTU) within the refinery complex, where it typically undergoes Wet Air Oxidation (WAO) to safely convert the toxic sulfides into benign aqueous sodium sulfate (Na_2SO_4). Alternatively, the bulk of the recovered H_2S vapor is routed to a central Amine Regeneration Unit and subsequently to a Claus Plant, where the dangerous gas is catalytically converted into safe, elemental solid sulfur.

Following successful pretreatment, the sweetened naphtha is evaluated for downstream upgrading. Reforming lighter cuts is not economically viable due to their tendency to decompose and convert into lighter gases. Additionally, hydrocarbons with boiling points above 210 °C are not suitable due to cracking and excessive carbon (coke) production.

Sulfur is primarily present in the raw feedstock as organic compounds such as mercaptans, sulfides, and thiophenes. If these sulfur compounds are not removed, they poison and deactivate downstream catalysts. Furthermore, upon combustion of the final fuel, these compounds are oxidized to form sulfur oxides (SOx), which are major contributors to acid rain and air pollution (Haruna et al., 2025). Therefore, to produce clean fuel and achieve a sulfur content between 10 and 15 ppm, sulfur compounds must be thoroughly removed (Samimi, 2025). To meet these increasingly stringent global mandates, refineries must optimize their purification units. There are several reasons why it is necessary to desulfurize petroleum products, gas condensates, and hydrocarbon streams. In addition to mitigating environmental damage and air pollution, the desulfurization of distillates produced from primary distillation processes is also carried out for critical technical and economic reasons. Desulfurization is executed on an industrial scale via the hydrodesulfurization (HDS) process. While the general hydrotreating of heavier fractions (such as diesel) often requires extreme pressures that lead to the non-selective hydrogenation of aromatic rings (hydrodearomatization), Naphtha Hydrotreating (NHT) prior to catalytic reforming requires strict thermodynamic selectivity. In the proposed NHT simulation, the operating conditions are strictly optimized to balance desulfurization with octane preservation. Highly reactive unsaturated compounds (olefins) are readily targeted and saturated by the hydrogen feed, which is a necessary kinetic pathway to prevent rapid coking and fouling on the downstream reforming catalyst. However, because aromatic rings are highly stabilized by resonance, their saturation requires crossing a much higher thermodynamic activation barrier. By strictly managing the reactor temperature and maintaining the hydrogen partial pressure below this specific threshold, the proposed unit selectively cleaves carbon-sulfur bonds (HDS) without hydrogenating the stable aromatic compounds. This precise thermodynamic control ensures deep desulfurization while fully preserving the valuable aromatic precursors essential for maximizing the final reformate octane number.

5. Conclusion

The simulation of refinery processes, specifically Naphtha Hydro-Treating (NHT) and continuous Catalytic Reforming using Aspen HYSYS, serves as an indispensable tool for chemical engineers in predicting unit performance and optimizing design parameters. This study confirms that the Naphtha Hydro-Treating (NHT) process is essential for protecting downstream catalysts from poisoning caused

by sulfur, nitrogen, oxygen, and metallic contaminants. Achieving a sulfur concentration of less than 0.5 ppm in the light naphtha fraction is a critical industrial benchmark for high-quality gasoline production, and this is effectively modeled through catalytic desulfurization in a hydrogen-rich environment.

The simulation results provide key insights into the performance of the reaction section. While variations in operating pressure showed a negligible impact on the mass flow rates of H_2S and CO_2 exciting the three-phase flash, temperature adjustments significantly influenced phase distribution. In accordance with thermodynamic principles, increasing the system temperature led to a decrease in liquid-phase mass flow and a corresponding increase in the vapor-phase flow rate. Notably, at temperatures reaching 90°C, the concentration of mercaptans in the vapor phase exiting the catalytic reactors increased. While the recovery of mercaptans in the flash units decreased at higher temperatures due to shifted equilibrium, the total output of H_2S and CO_2 remained relatively constant. Ultimately, this study demonstrates that while temperature is a critical variable for mercaptan distribution, the removal of acid gases (H_2S and CO_2) within the flash separation stages remains stable across the tested pressure and temperature ranges, validating the reliability of the NHT unit design under varying thermal conditions.

CRediT Author Contribution Statement

Hussam Elddin Nabeih Khasawneh: Conceptualization of the study, process simulation, and writing the original draft of the manuscript.
Nada Al-Ananzeh: Contributed to the formal data analysis and the critical review of the manuscript.
Fares Abu Affan: Responsible for validation and editing during the peer-review revision process.

Declaration Statements

Funding
This research received no external funding.

Conflicts of Interest
The authors declare no conflict of interest.

Nomenclature

Appreviation	Full Term
A	Surface area
ASTM	American Society for Testing and Materials
Bio-DS	Biological Desulfurization
CCR	Continuous Catalytic Regeneration
DOC	Diesel Oxidation Catalyst
DPF	Diesel Particulate Filter
EDS	Extractive Desulfurization
EPA	Environmental Protection Agency (United States)
HDN	Hydrodenitrogenation
HDS	Hydrodesulfurization
IMO	International Maritime Organization
LSD	Low-Sulfur Diesel
MEPC	Marine Environment Protection Committee
NHT	Naphtha Hydrotreating
ODS	Oxidative Desulfurization
OSBL	Outside Battery Limits
PM	Particulate Matter
PONA	Paraffins, Olefins, Naphthenes, Aromatics

References

Abubakar, U. C., Alhooshani, K. R., & Saleh, T. A. (2020). Effect of ultrasonication and chelating agents on the dispersion of NiMo catalysts on carbon for hydrodesulphurization. *Journal of Environmental Chemical Engineering, 8*(3), Article 103811. https://doi.org/10.1016/j.jece.2020.103811

Al-Ananzeh, N., Khasawneh, H., Al-Bodour, A., & Dawagreh, A.-K. (2025). Investigating the role of carboxymethyl cellulose and polyvinyl alcohol additives on concrete performance: A case study from Jordan. *Jordanian Journal of Engineering and Chemical Industries, 8*(1), 50–59. https://doi.org/10.48103/jjeci852025

Dastnaei, P. G. (2025). Investigation of 3D-printed polymers: A focus on material selection, processing methods, and emerging applications and potentials: Mini review. *Journal of Chemical Engineering and Energy Materials, 1*(3), 156–166. https://doi.org/10.22034/jceem.2025.544001.1019

Gandomi, M. J. (2024). Exploring novel catalysts for enhanced CO_2 reduction reactions. *Eurasian Journal of Chemical, Medicinal and Petroleum Research, 3*(4), 1321–1332. https://doi.org/EJCMPR/4225886

Gavanaroudi, S. B. (2024). Photocatalytic degradation of organic pollutants under visible light irradiation. *Eurasian Journal of Chemical, Medicinal and Petroleum Research, 3*(5), 18–32. https://doi.org/EJCMPR/4221486

Ghanbari Pakdehi, S., Bahri, M., & Shirmohammadi, M. (2025). Optimizing the catalytic transfer hydrogenation of naphthalene to tetralin via response surface methodology. *Iranian Journal of Chemistry and Chemical Engineering, 44*, 837–845. https://doi.org/10.30492/ijcce.2025.2037748.6732

Han, K. L. (2022). Investigation of thermal and catalytic pyrolysis of polyolefin and rubbers. *Eurasian Journal of Chemical, Medicinal and Petroleum Research, 1*(4), 120–129.

Han, W., Nie, H., Long, X., Li, M., Yang, Q., & Li, D. (2017). Effects of the support Brønsted acidity on the hydrodesulfurization and hydrodenitrogenation activity of sulfided NiMo/Al_2O_3 catalysts. *Catalysis Today, 292*, 58–66. https://doi.org/10.1016/j.cattod.2016.11.049

Haruna, A., Merican, Z. M. A., Juma, A. K., Aliero, A. S., Ekeoma, B. C., Abdullahi, M., Imam, M., Abdulsalam, S., & Hamza, S. A. (2025). Fuel desulfurization using ionic liquids: An updated review. *Journal of Ionic Liquids, 5*(2), Article 100162. https://doi.org/10.1016/j.jil.2025.100162

Imanzadeh, M. (2024). Mechanistic studies of organic-metallic catalysts in cross-coupling reactions. *Eurasian Journal of Chemical, Medicinal and Petroleum Research, 3*(5), 86–93.

Khasawneh, H. E. N. (2025). Review of studies on refinery unit simulation. *Journal of Chemical Reviews, 7*, 512–530. https://doi.org/10.48309/JCR.2025.517153.1443

Khasawneh, H. E. N., Ameer, S. A., Qassem, L. Y., Hussein, A. H. A., Saud, H. R., Idan, A. H., Bahair, H., & Samimi, A. (2025). Examining the design parameters of solvents of carbon dioxide production unit using diesel combustion method. *Iranian Journal of Chemistry and Chemical Engineering, 44*(1), 235–243. https://doi.org/10.30492/IJCCE.2024.2026782.6550

Khasawneh, H. E. N., Sharifi Tashnizi, S. H., Hanif, H. R., & Aflaki, S. (2025). Design and calculation of a chlorinated container to prevent oil production. *Chemical Methodologies, 9*, 190–207. https://doi.org/10.48309/CHEMM.2025.500944.1885

Khosravanipour Mostafazadeh, A., & Rahimpour, M. R. (2009). A membrane catalytic bed concept for naphtha reforming in the presence of catalyst deactivation. *Chemical Engineering and Processing: Process Intensification, 48*(2), 683–694. https://doi.org/10.1016/j.cep.2008.08.003

Martins, M., Smoliło-Utrata, M., Tarach, K. A., Samson, K., Gackowski, M., Madej, E., Korecki, J., Mordarski, G., Śliwa, M., Jarczewski, S., Podobiński, J., Kuśtrowski, P. K., Datka, J., Rutkowska-Zbik, D., & Góra-Marek, K. (2022). Modulation of ODH propane selectivity by zeolite support desilication: Vanadium species anchored to Al-rich shell as crucial active sites. *International Journal of Molecular Sciences*, 23(10), 5584. https://doi.org/10.3390/ijms23105584

Mahdiraji, E. A., & Zarini, M. K. (2025). Advanced material-based cooling and insulation strategies for enhanced protection of synchronous generators under fault conditions. *Journal of Chemical Engineering and Energy Materials, 1*(3), 119–125. https://doi.org/10.22034/JCEEM.2025.542846.1011

Mehrdadian, M. M. (2025). Process design of vinyl chloride monomer production by Aspen Plus. *Journal of Chemical Engineering and Energy Materials, 1*(4), 191–199. https://doi.org/10.22034/jceem.2025.547239.1020

Mevawala, C., Bai, X., Hu, J., & Bhattacharyya, D. (2023). Plant-wide modeling and techno-economic analysis of a direct non-oxidative methane dehydroaromatization process via conventional and microwave-assisted catalysis. *Applied Energy, 336*, Article 120795. https://doi.org/10.1016/j.apenergy.2023.120795

Mouler, T. (2025). A review of polymerization techniques for preparing hydrogels. *Journal of Chemical Engineering and Energy Materials, 1*(3), 126–134. https://doi.org/10.22034/jceem.2025.543012.1016

Noorpoor, A. R., & Mazare, F. (2018). Conventional and advanced exergetic and exergoeconomic analysis applied to an air preheater system for fired heater (Case study: Tehran Oil Refinery Company). *Iranian Journal of Chemistry and Chemical Engineering, 37*(4), 205–219. https://doi.org/10.30492/IJCCE.2018.28879

Overhary, M. (2025). Exploring the role of technological progress in reducing carbon emissions. *Journal of Chemical Engineering and Energy Materials, 1*(3), 135–142. https://doi.org/10.22034/jceem.2025.543015.1017

Padervand, M., Lammel, G., Bargahi, A., & Mohammad-Shiri, H. (2019). Photochemical degradation of the environmental pollutants over the worm-like Nd_2CuO_4–Nd_2O_3 nanostructures. *Nano-Structures & Nano-Objects, 18*, 100258. https://doi.org/10.1016/j.nanoso.2019.100258

Padervand, M., Rhimi, B., & Wang, C. (2021). One-pot synthesis of novel ternary $Fe_3N/Fe_2O_3/C_3N_4$ photocatalyst for efficient removal of Rhodamine B and CO_2 reduction. *Journal of Alloys and Compounds, 852*, 156955. https://doi.org/10.1016/j.jallcom.2020.156955

Pershima, N. (2025). Feasibility study of biodegradation of gaseous pollutants with respect to industrial processes. *Journal of Chemical Engineering and Energy Materials, 1*(3), 143–155. https://doi.org/10.22034/jceem.2025.543074.1018

Samimi, A. (2025). Investigating the effect of temperature and pressure changes in CCR unit reactors on catalyst wear and black dust increase. *Iranian Journal of Chemistry and Chemical Engineering, 44*(12), 3039–3051. https://doi.org/10.30492/IJCCE.2025.2067307.7221

Samimi, A., & Zarinabadi, S. (2011). Reduction of greenhouse gases emission and effect on environment. *Australian Journal of Basic and Applied Sciences, 5*(12), 752–756.

Samimi, A., & Zarinabadi, S. (2012). Application polyurethane as coating in oil and gas pipelines. In *CHISA 2012: 20th International Congress of Chemical and Process Engineering and PRES 2012: 15th Conference on Process Integration, Modelling and Optimisation for Energy Saving and Pollution Reduction*. Prague, Czech Republic.

Samimi, A., Zarinabadi, S., Shahbazi Kootenaei, A. H., Azimi, A., & Mirzaei, M. (2019). Use of data mining in the corrosion classification of pipelines in catalytic reforming units (CRU). *Eurasian Chemical Communications, 1*(6), 571–581.

Samimi, A., Zarinabadi, S., Shahbazi Kootenaei, A. H., Azimi, A., & Mirzaei, M. (2020). Corrosion classification of pipelines in hydrocracking units (ISOMAX) by data mining. *South African Journal of Chemical Engineering, 31*, 44–50. https://doi.org/10.1016/j.sajce.2019.11.006

Vakili, F. (2025). Investigation of corrosion conditions in naphtha hydro treating (NHT) units: A data-based analysis. *Journal of Chemical Engineering and Energy Materials, 1*(4), 176–190. https://doi.org/10.22034/JCEEM.2025.550999.1021